Stable weak-light ultraslow spatiotemporal solitons via atomic coherence

Hui-jun Li,[1,*] Yuan-po Wu,[1] and Guoxiang Huang[2,†]

[1]*Institute of Nonlinear Physics, Zhejiang Normal University, Jinhua, 321004 Zhejiang, China*
[2]*State Key Laboratory of Precision Spectroscopy, East China Normal University, 200062 Shanghai, China*

We propose a scheme to generate stable ultraslow three-dimensional spatiotemporal optical solitons, or ultraslow optical bullets, at very low light levels via atomic coherence. The system we consider is an ensemble of resonant, lifetime-broadened N-type four-level atoms, working in a regime of electromagnetically induced transparency. Due to the quantum interference effect induced by a control field, the absorption of a probe field is largely suppressed. Moreover, the Kerr nonlinearity is greatly enhanced, and the dispersion property of the probe field is drastically changed. Using a method of multiple scales, we derive two coupled nonlinear envelope equations controlling the evolution of the envelopes of the probe field and an assisted field. We show that under certain conditions the envelope of the probe field satisfies a three-dimensional nonlinear Schrödinger equation and the envelope of the assisted field obeys a linear Helmholtz equation. We obtain various optical bullet solutions for the probe-field envelope and demonstrate that such optical bullets have many novel features, including very slow propagating velocity and very low generation power. In addition, they can be actively controlled and manipulated by adjusting system parameters. The stabilization of the optical bullets obtained can be easily realized by the trapping potential contributed by the assisted field, which is also investigated in detail.

I. INTRODUCTION

In past two decades, there has been intensive study on optical wave packets that are localized in all three spatial dimensions as they propagate in space and evolve in time. These wave packets, called spatiotemporal optical solitons or optical bullets [1], appear as a result of the interplay between dispersion, diffraction, and nonlinearity. Optical bullets are of great interest due to their rich nonlinear physics and important applications [2–22]. However, up to now most optical bullets are produced in passive optical media, in which faroff resonance excitation schemes are employed in order to avoid significant optical absorption. Moreover, for generating the optical bullets in passive optical media, very high light intensity is usually needed to obtain nonlinearity strong enough to balance dispersion and diffraction effects. In addition, in passive media an active control on the property of optical bullets is hard to realize because there is no energy-level structure and selection rules that can be used and manipulated.

For practical applications, the optical bullets having low generation power and good controllability are desirable. Active optical media, in which light interacts with matter resonantly, can be used to achieve such goal. However, for on-resonance media there is usually a very large optical absorption. In recent years, such a paradigm has been changed by the finding of electromagnetically induced transparency (EIT) in resonant atomic systems. Due to the quantum interference effect induced by an additional control field, the propagation of a weak probe field displays many striking features, including a significant suppression of optical absorption, a large reduction of probe-field group velocity, and a giant enhancement of Kerr nonlinearity [23]. Based on these important features, it has

been suggested recently that new types of temporal [24–27] and spatial [28–31] optical solitons are possible in highly resonant atomic systems.

In this article, we propose a scheme to generate three-dimensional (3D) optical bullets in an active optical medium via quantum coherence. The system we consider is an ensemble of resonant, lifetime-broadened four-level atoms, working in an EIT regime and at low temperature. By the use of the EIT effect induced by a continuous-wave (CW) control field, the absorption of a weak probe pulse can be largely suppressed. Simultaneously, the Kerr nonlinearity is greatly enhanced and the dispersion property of the probe pulse is drastically changed, which are used to form 3D optical bullets in the system. Using a standard method of multiple scales, we derive two coupled nonlinear envelope equations governing the spatiotemporal evolution of the probe field and an assisted field. We show that under some conditions the envelope equation of the probe field can be reduced into a $(3 + 1)$-dimensional $[(3 + 1)D]$ [32] nonlinear Schrödinger (NLS) equation and the envelope of the assisted field obeys a linear Helmholtz equation. We obtain various optical bullet solutions for the probe-field envelope and demonstrate that the optical bullets suggested in the present active system are very different from those in passive systems obtained before [1–19], and possess many novel features, including: (i) They have ultraslow propagating velocity ($\sim 10^{-5}c$; c is the light speed in a vacuum). (ii) Their generation power is very low ($\leqslant 1\,\mu W$). (iii) They can be actively controlled and manipulated based on the active characters of the system. Especially, the signs of the Kerr nonlinearity and dispersion can be manipulated at will by, for example, adjusting detunings and pulse length. (iv) They can be stabilized easily by using the assisted CW laser field, or a pulsed assisted field with a suitable time length, which provides an "external" potential acting on the optical bullets, hence stabilizing their propagation. The stable and controllable weak-light ultraslow optical bullets via atomic

*Corresponding author:hjli@zjnu.cn

†Corresponding author:gxhuang@phy.ecnu.edu.cn

coherence obtained here may have potential applications in optical information processing and transmission.

The article is arranged as follows. In the next section, we give an introduction of the model under study. In Sec. III, using a method of multiple scales we derive two coupled nonlinear equations for the envelopes of the probe and the assisted fields, and discuss under what condition these envelope equations can be reduced to a $(3 + 1)$D nonlinear NLS equation and a linear Helmholtz equation. In Sec. IV, we investigate the formation and propagation of the 3D optical bullets and discuss their stability in detail. In the final section, we summarize the main results obtained in our work.

II. MODEL

We consider a cold, lifetime-broadened atomic system with an N-type energy-level configuration, as shown in Fig. 1. A weak pulsed probe field (strong CW control field) with center angular frequency ω_p (ω_c) and half Rabi frequency Ω_p (Ω_c) interacts resonantly with the energy states $|1\rangle$ and $|3\rangle$ ($|2\rangle$ and $|3\rangle$). The energy states $|1\rangle$, $|2\rangle$, and $|3\rangle$ together with the probe and control fields consist of a widely studied Λ-type three-level EIT core. In addition, a weak assisted laser field with center angular frequency ω_a (half Rabi frequency Ω_a) couples to energy states $|2\rangle$ and $|4\rangle$, which contributes a cross-phase modulation (CPM) to the probe field. We take the energy levels from the D_2 line of ^{87}Rb atoms, with
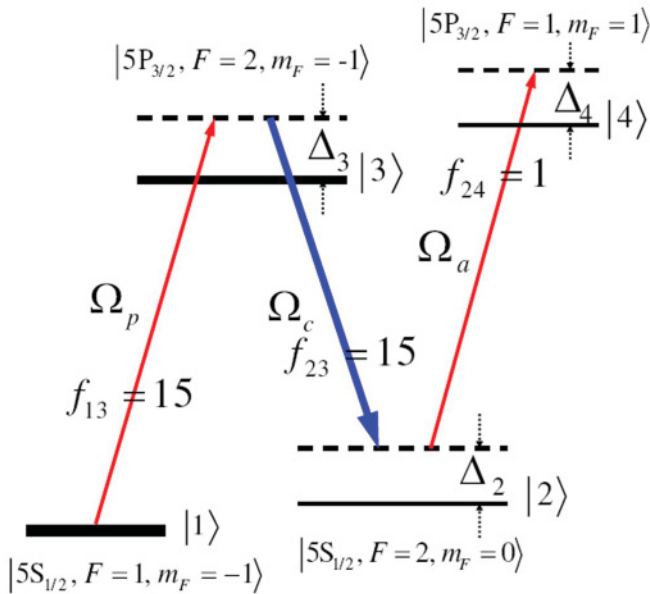

FIG. 1. (Color online) Energy-level diagram and excitation scheme of the lifetime-broadened four-state atomic system interacting with a weak pulsed probe field (with half Rabi frequency Ω_p), a strong CW control field (with half Rabi frequency Ω_c), and a weak assistant field (with half Rabi frequency Ω_a). Δ_3, Δ_2, and Δ_4 are one-photon, two-photon, and three-photon detunings, respectively. The energy levels are taken from the D_2 line of ^{87}Rb atoms, with $|1\rangle = |5S_{1/2}, F = 1, m_F = -1\rangle$, $|2\rangle = |5S_{1/2}, F = 2, m_F = 0\rangle$, $|3\rangle = |5P_{3/2}, F = 2, m_F = -1\rangle$, and $|4\rangle = |5P_{3/2}, F = 1, m_F = 1\rangle$. $f_{ij} = |\mathbf{p}_{ij}/D_2|^2 \times 120$ is the relative transition strength, with $D_2 = 3.58 \times 10^{-27}$ cm C and $\mathbf{p}_{ij}$ being the dipole transition matrix element between the state $|i\rangle$ and the state $|j\rangle$.

the states selected as $|1\rangle = |5S_{1/2}, F = 1, m_F = -1\rangle$, $|2\rangle = |5S_{1/2}, F = 2, m_F = 0\rangle$, $|3\rangle = |5P_{3/2}, F = 2, m_F = -1\rangle$, and $|4\rangle = |5P_{3/2}, F = 1, m_F = 1\rangle$. f_{ij} in the figure is the relative transition strength, defined by $f_{ij} = |\mathbf{p}_{ij}/D_2|^2 \times 120$, where $D_2 = 3.58 \times 10^{-27}$ cm C and $\mathbf{p}_{ij}$ is the dipole transition matrix element between the state $|i\rangle$ and the state $|j\rangle$ [33].

The electric-field vector in the system can be written as $\mathbf{E} = \sum_{l=p,c,a} \mathbf{e}_l \mathcal{E}_l \exp[i(\mathbf{k}_l \cdot \mathbf{r} - \omega_l t)] + \text{c.c.}$, where $\mathbf{e}_l$ ($\mathbf{k}_l$) is polarization direction (wave vector) of lth field with envelope $\mathcal{E}_l$. The Hamiltonian of the system is given by $\hat{H} = \hat{H}_0 + \hat{H}'$, where $\hat{H}_0$ and $\hat{H}'$ describe a free atom and the interaction between the atom and the electric field, respectively. Our theoretical model is based on the density matrix equation for the four-level atoms together with the Maxwell equations for the weak laser fields. In the Schrödinger picture, the state vector of the system is $|\Psi(t)\rangle = \sum_{j=1}^{4} a_j |j\rangle$, where $|j\rangle$ is the eigenvector of $\hat{H}_0$ with eigenenergy $\hbar\omega_j$, and a_j is the probability amplitude of the state $|j\rangle$. Under electric-dipole and rotating-wave approximations, the Hamiltonian reads $\hat{H} = \sum_{j=1}^{4} \hbar\omega_j |j\rangle\langle j| - \hbar(\Omega_p e^{i(\mathbf{k}_p \cdot \mathbf{r} - \omega_p t)}|3\rangle\langle 1| + \Omega_c e^{i(\mathbf{k}_c \cdot \mathbf{r} - \omega_c t)}|3\rangle\langle 2| + \Omega_a e^{i(\mathbf{k}_a \cdot \mathbf{r} - \omega_a t)}|4\rangle\langle 2| + \text{H.c.})$, with $\Omega_p \equiv (\mathbf{e}_p \cdot \mathbf{p}_{13})\mathcal{E}_p/\hbar$, $\Omega_c \equiv (\mathbf{e}_c \cdot \mathbf{p}_{23})\mathcal{E}_c/\hbar$, and $\Omega_a \equiv (\mathbf{e}_a \cdot \mathbf{p}_{24})\mathcal{E}_a/\hbar$, and H.c. being the Hermitian conjugate.

By making the transformation $a_j = A_j \exp[i(\mathbf{k}_j \cdot \mathbf{r} - \omega_j t - \Delta_j t)]$, with $\Delta_1 = 0$, $\mathbf{k}_1 = 0, \mathbf{k}_2 = \mathbf{k}_p - \mathbf{k}_c, \mathbf{k}_3 = \mathbf{k}_p$, and $\mathbf{k}_4 = \mathbf{k}_p - \mathbf{k}_c + \mathbf{k}_a$, we obtain the Hamiltonian in the interaction picture $\hat{H}_{\text{int}} = -\hbar \sum_{j=1}^{4} \Delta_j |j\rangle\langle j| - \hbar(\Omega_p|3\rangle\langle 1| + \Omega_c|3\rangle\langle 2| + \Omega_a|4\rangle\langle 2| + \text{H.c.})$, where $\Delta_3 = \omega_p - (\omega_3 - \omega_1), \Delta_2 = \omega_p - \omega_c - (\omega_2 - \omega_1)$, and $\Delta_4 = \omega_p - \omega_c + \omega_a - (\omega_4 - \omega_1)$ are the one-, two-, and three-photon detunings, respectively. The equation of motion of the density matrix σ (with the matrix element defined by $\sigma_{ij} = A_i A_j^*$) in the interaction picture reads

$$\frac{\partial \sigma}{\partial t} = -\frac{i}{\hbar}[\hat{H}_{\text{int}}, \sigma] - \Gamma(\sigma), \tag{1}$$

where $\Gamma(\sigma)$ is a 4×4 relaxation matrix. Explicit expressions of the equations of motion for σ_{ij} have been given in the Appendix A.

The electric-field evolution is controlled by Maxwell equation $\nabla^2 \mathbf{E} - (1/c^2)\partial^2 \mathbf{E}/\partial t^2 = (1/\epsilon_0 c^2)\partial^2 \mathbf{P}/\partial t^2$, where $\mathbf{P} = N(\mathbf{p}_{13}\sigma_{31}\exp[i(\mathbf{k}_3 \cdot \mathbf{r} - \omega_p t)] + \mathbf{p}_{23}\sigma_{32}\exp\{i[(\mathbf{k}_3 - \mathbf{k}_2) \cdot \mathbf{r} - \omega_c t]\} + \mathbf{p}_{24}\sigma_{42}\exp\{i[(\mathbf{k}_4 - \mathbf{k}_2) \cdot \mathbf{r} - \omega_a t]\}) + \text{c.c.}$. Under a slowly varying envelope approximation, the Maxwell equation is reduced to

$$i\left(\frac{\partial}{\partial z} + \frac{1}{c}\frac{\partial}{\partial t}\right)\Omega_p + \frac{c}{2\omega_p}\left(\frac{\partial^2}{\partial x^2} + \frac{\partial^2}{\partial y^2}\right)\Omega_p + \kappa_{13}\sigma_{31} = 0, \tag{2a}$$

$$i\left(\frac{\partial}{\partial z} + \frac{1}{c}\frac{\partial}{\partial t}\right)\Omega_a + \frac{c}{2\omega_a}\left(\frac{\partial^2}{\partial x^2} + \frac{\partial^2}{\partial y^2}\right)\Omega_a + \kappa_{24}\sigma_{42} = 0, \tag{2b}$$

where $\kappa_{13,24} = N\omega_{p,a}|\mathbf{e}_{p,a} \cdot \mathbf{p}_{13,24}|^2/(2\epsilon_0\hbar c)$, with N being the atomic concentration. For simplicity, the probe field and the assistant field have been assumed to propagate in z direction, i.e., $\mathbf{k}_{p,a} = \mathbf{e}_z k_{p,a}$.

III. ASYMPTOTIC EXPANSION AND (3 + 1)D NONLINEAR ENVELOPE EQUATIONS

Although a lot of research on the system shown in Fig. 1 exists [23,34], most of these projects are designed for the linear and steady-state solution. Here we are interested in the nonlinear evolution and the possible formation of optical bullets in the system. For this aim we employ the standard method of multiple scales that is well developed in nonlinear wave theory [35] to investigate the evolution of both the probe and assisted fields. We assume that the atoms are initially populated in state $|1\rangle$. We make the asymptotic expansions $\sigma_{ij} = \sigma_{ij}^{(0)} + \epsilon\sigma_{ij}^{(1)} + \epsilon^2\sigma_{ij}^{(2)} + \epsilon^3\sigma_{ij}^{(3)} + \cdots$, and $\Omega_{p,a} = \epsilon\Omega_{p,a}^{(1)} + \epsilon^2\Omega_{p,a}^{(2)} + \epsilon^3\Omega_{p,a}^{(3)} + \cdots$, with $\sigma_{ij}^{(0)} = \delta_{i1}\delta_{j1}$. Here ϵ is a small parameter characterizing the typical amplitude of the probe and assisted fields. To obtain divergence-free expansions, all quantities on the right hand sides of the asymptotic expansions are considered as functions of the multiscale variables $z_l = \epsilon^l z$ $(l = 0,1,2)$, $t_l = \epsilon^l t$ $(l = 0,1)$, $x_1 = \epsilon x$, and $y_1 = \epsilon y$. Substituting these expansions into Eqs. (A1) and (2), one can obtain a series of linear but inhomogeneous equations for $\sigma_{ij}^{(l)}$ and $\Omega_{p,a}^{(l)}$ $(l = 1,2,3,\ldots)$, which can be solved order by order.

At the first order, we obtain the solution under linear level

$$\Omega_p^{(1)} = F\,e^{i\theta}, \tag{3a}$$

$$\Omega_a^{(1)} = G, \tag{3b}$$

$$\sigma_{31}^{(1)} = \frac{\omega + d_{21}}{D}Fe^{i\theta}, \tag{3c}$$

$$\sigma_{21}^{(1)} = -\frac{\Omega_c^*}{D}Fe^{i\theta}, \tag{3d}$$

with $D = |\Omega_c|^2 - (\omega + d_{21})(\omega + d_{31})$ [36], and other $\sigma_{ij}^{(1)}$ being zero. In the above expressions, $\theta = K(\omega)z_0 - \omega t_0$, and F and G are yet to be determined envelope functions depending on the slow variables t_1, z_1, and z_2. We see that in this order the evolutions of both fields are independent. Moreover, the assisted field is free, but the probe field experiences a dispersion and absorption (contributed by the Λ-type three-level EIT core) with the linear dispersion relation given by

$$K(\omega) = \frac{\omega}{c} + \frac{\kappa_{13}(\omega + d_{21})}{D}. \tag{4}$$

Shown in Fig. 2 are the imaginary part $\mathrm{Im}K(\omega)$ [panel (a)] and the real part $\mathrm{Re}K(\omega)$ [panel (b)] of $K(\omega)$ as functions of dimensionless frequency ω/Γ_3. The system parameters used are $\Gamma_1 = \Delta_1 = 0\,\mathrm{Hz}$, $\Gamma_2 = 1 \times 10^3\,\mathrm{Hz}$, $\Gamma_3 = 35\,\mathrm{MHz}$, $\kappa_{13} = 1.0 \times 10^{10}\,\mathrm{cm}^{-1}\mathrm{s}^{-1}$, and $\Delta_{2,3} = -1.5 \times 10^6\,\mathrm{s}^{-1}$. The dashed-dotted and the solid lines in both panels correspond to the presence $(\Omega_c = 5 \times 10^7\ \mathrm{s}^{-1})$ and the absence $(\Omega_c = 0)$ of the control field, respectively. One sees that when Ω_c is absent, the probe field has a large absorption [the solid line of panel (a)]; however, when Ω_c is applied, a transparency window is opened [the dashed-dotted line of panel (a)]. The steep slope for the large control field [the dashed-dotted line
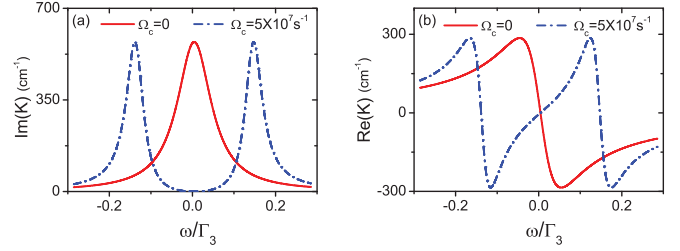

FIG. 2. (Color online) Imaginary part $\mathrm{Im}K(\omega)$ [panel (a)] and the real part $\mathrm{Re}K(\omega)$ [panel (b)] of the linear dispersion relation of the probe field as functions of dimensionless frequency ω/Γ_3. In both panels, the dashed-dotted and solid lines correspond to the presence $(\Omega_c = 5 \times 10^7\ \mathrm{s}^{-1})$ and the absence $(\Omega_c = 0)$ of the control field, respectively. A transparency window is opened for the large control field [the dotted-dashed line in panel (a)]. The steep slope of the dashed-dotted line for the large control field [the dotted-dashed line in panel (b)] results in a slow group velocity.

of panel (b)] results in a slow group velocity at the center frequency of the probe field (i.e., $\omega = 0$):

$$V_g \equiv \left(\frac{\partial K}{\partial \omega}\right)^{-1} = 8.31 \times 10^{-6}c. \tag{5}$$

The suppression of the absorption and the reduction of the group velocity are due to the quantum interference effect induced by the control field.

At the second order, the solvability condition for $\sigma_{ij}^{(2)}$ and $\Omega_{p,a}^{(2)}$ requires

$$i\left(\frac{\partial}{\partial z_1} + \frac{1}{V_g}\frac{\partial}{\partial t_1}\right)F = 0, \tag{6a}$$

$$i\left(\frac{\partial}{\partial z_1} + \frac{1}{c}\frac{\partial}{\partial t_1}\right)G = 0. \tag{6b}$$

Equation (6) means that up to the second order the evolutions of the probe field and that of the assisted field are still independent of each other.

At the third order, using the solvability condition for $\sigma_{ij}^{(3)}$ and $\Omega_{p,a}^{(3)}$, we obtain the coupled nonlinear equations for F and G:

$$i\frac{\partial}{\partial z_2}F + \frac{c}{2\omega_p}\left(\frac{\partial^2}{\partial x_1^2} + \frac{\partial^2}{\partial y_1^2}\right)F - \frac{1}{2}K_2\frac{\partial^2 F}{\partial t_1^2}$$
$$+ \alpha_{11}|F|^2F + \alpha_{12}|G|^2F = 0, \tag{7a}$$

$$i\frac{\partial}{\partial z_2}G + \frac{c}{2\omega_a}\left(\frac{\partial^2}{\partial x_1^2} + \frac{\partial^2}{\partial y_1^2}\right)G + \alpha_{21}|F|^2G = 0, \tag{7b}$$

where $K_2 = \partial^2 K/\partial\omega^2$. The explicit expressions for the coefficient of self-phase modulation (SPM) of the probe field (i.e., α_{11}), and the coefficients of cross-phase modulation (CPM) between the two fields (i.e., α_{12} and α_{21}) are given in the Appendix B.

Now we make some remarks on Eqs. (6) and (7). From Eq. (6) we know that the probe-field envelope F travels with group velocity V_g, whereas the assisted-field envelope G travels with velocity c. Thus the two wave fields will separate from each other when traveling to a large propagating distance. In this case, Eq. (7a) reduces to a (3 + 1)D NLS equation for F,

allowing an optical bullet solution. However, such an optical bullet solution is unstable [1–5]. To obtain stable optical bullets we make the following assumptions: (i) The assisted field is a stationary one (i.e., G is independent of t_1 and hence also independent of z_1), or it is a pulsed field but with a enough large time length [37] so that the derivatives $\partial/\partial t_1$ and $\partial/\partial z_1$ in Eq. (6b) can be neglected. In the both cases the assisted field is (or can be approximated as) a CW beam and so the probe field can interact with the assisted field for a long time. (ii) If we select the atomic transition between $|2\rangle$ and $|4\rangle$ to be relatively weak compared to those between $|1\rangle$ and $|3\rangle$ and between $|2\rangle$ and $|3\rangle$, the coupling constants in Eqs. (2a) and (2b) satisfy $\kappa_{24} \ll \kappa_{13}$, and hence $\alpha_{21} \ll \alpha_{11}, \alpha_{12}$. In this way the CPM term in Eq. (7b) can be safely neglected. In fact, we have made such a selection in our model shown in Fig. 1, in which the transition strength between $|2\rangle$ and $|4\rangle$ is much less the transition strength between $|1\rangle$ and $|3\rangle$ and between $|2\rangle$ and $|3\rangle$, i.e., $f_{24} \ll f_{13}, f_{23}$. Under these conditions, Eq. (7) is reduced into a linear Helmholtz equation. As a result, by combining Eqs. (6) and (7) we obtain the following simplified envelope equations:

$$i\left(\frac{\partial}{\partial z} + \frac{1}{V_g}\frac{\partial}{\partial t}\right)U + \frac{c}{2\omega_p}\left(\frac{\partial^2}{\partial x^2} + \frac{\partial^2}{\partial y^2}\right)U - \frac{1}{2}K_2\frac{\partial^2 U}{\partial t^2}$$
$$+ \alpha_{11}|U|^2 U + \alpha_{12}|V|^2 U = 0, \tag{8a}$$

$$i\frac{\partial V}{\partial z} + \frac{c}{2\omega_a}\left(\frac{\partial^2}{\partial x^2} + \frac{\partial^2}{\partial y^2}\right)V = 0, \tag{8b}$$

after returning to the original variables, where $U = \epsilon F$ and $V = \epsilon G$. One sees that the role of the assisted field envelope G is now to provide just an external potential [controlled by the linear Helmholtz Eq. (8b)] to the probe field envelope F [controlled by the (3 + 1)D NLS Eq. (8a)]. This is desirable since the external potential G can be used to stabilize the optical bullets formed in the envelope F of the probe field, as shown below.

IV. OPTICAL BULLETS AND THEIR STABILITY

A. Estimation on the coefficients in the coupled envelope equations

We now explore possible optical bullet solutions based on the Eqs. (8a) and (8b). For convenience, we convert them into the dimensionless form

$$i\frac{\partial u}{\partial s} + \frac{1}{2}\left(\frac{\partial^2}{\partial \xi^2} + \frac{\partial^2}{\partial \eta^2} + g_d\frac{\partial^2}{\partial \tau^2}\right)u + g_{11}|u|^2 u$$
$$+ g_{12}|v|^2 u = 0, \tag{9a}$$
$$i\frac{\partial v}{\partial s} + \frac{\delta}{2}\left(\frac{\partial^2}{\partial \xi^2} + \frac{\partial^2}{\partial \eta^2}\right)v = 0, \tag{9b}$$

with $u = U/U_0$, $v = V/(U_0 c_0)$, $s = z/L_{\text{diff}}, \tau = (t - z/V_g)/\tau_0$, $(\xi, \eta) = (x, y)/R_\perp$, $g_d = -L_{\text{diff}}K_2/\tau_0^2$, $g_{11} = \alpha_{11}/|\alpha_{11}|$, $g_{12} = \alpha_{12}c_0^2/|\alpha_{11}|$, and $\delta = \omega_p/\omega_a$. Here $L_{\text{diff}} \equiv \omega_p R_\perp^2/c$ (with $R_\perp$ being a typical beam radius) is a typical diffraction length, and τ_0 is a typical pulse length of the probe field. We have taken $L_{\text{diff}} = L_{NL}$ [with $L_{NL} = 1/(|\alpha_{11}U_0^2|)$ being a typical nonlinear length];

thus we have $U_0 = \sqrt{c/(\omega_p R_\perp^2 |\alpha_{11}|)}$ (a typical Rabi frequency of the probe field). Note that c_0 is proportional to a typical Rabi frequency of the assisted field, which is a free parameter that can be used to adjust the magnitude of the coefficient of the cross-phase modulation, and hence control the stability of the optical bullets.

Because the system under study is of resonant, lifetime-broadened character, the coefficients in the Eq. (9a) are generally complex. If the control field Rabi frequency Ω_c is small, the imaginary part of the coefficients is comparable with their real part, and hence stable optical bullet solutions do not exist. However, under the EIT condition $|\Omega_c|^2 \gg \gamma_{31}\gamma_{21}$ [38], the absorption of the probe field can be largely suppressed, and hence the imaginary part of these coefficients can be made to be much smaller than their real part.

To show this we make an estimation on the value of the coefficients in the Eqs. (9a) and (9b). Consider a typical atomic gas of ^{87}Rb atoms, with D_2 line transitions $5^2 S_{1/2} \to 5^2 P_{3/2}$. The energy levels are chosen as those in Fig. 1. From the data of ^{87}Rb [33], we have the dipole matrix elements $|\mathbf{p}_{13}| = -\sqrt{\frac{1}{8}} \times 3.58 \times 10^{-27}$ cm C and $|\mathbf{p}_{24}| = \sqrt{\frac{1}{120}} \times 3.58 \times 10^{-27}$ cm C. The other system parameters are given by $\Gamma_2 = 1 \times 10^3$ Hz, $\Gamma_{3,4} = 35$ MHz, $\kappa_{13} = 1.0 \times 10^{10}$ cm^{-1}s^{-1}, $\kappa_{24} = 1.0 \times 10^9$ cm^{-1}s^{-1}, $\omega_{p,a} = 2.37 \times 10^{15}$ s^{-1}, $R_\perp = 4.0 \times 10^{-3}$ cm, $\Omega_c = 5.0 \times 10^7$ s^{-1}, and $\Delta_3 = -3.0 \times 10^8$ s^{-1}, with $\Gamma_{31} \approx \Gamma_{32} = \Gamma_3/2$, $\Gamma_{42} = \Gamma_4$. Even if the above system parameters are chosen to be fixed, we still have other system parameters Δ_3, Δ_4, and τ_0 that can be chosen and adjusted in a fairly arbitrary domain, which can be used to obtain many different regimes, two of which are listed in the following:

Regime 1. $\Delta_2 = -1.5 \times 10^6$ s^{-1}, $\Delta_4 = -1.0 \times 10^9$ s^{-1}, $\tau_0 = 1.48 \times 10^{-6}$ s, $c_0 = 1.3$. We have $L_{\text{diff}} = 1.26$ cm, $U_0 = 9.0 \times 10^6$ s^{-1}, $V_g/c = 5.6 \times 10^{-6}$, and thus

$$\delta = 1.0, \quad g_d = 1.0 - 0.098i, \quad g_{11} = 1.0 - 0.018i,$$
$$g_{12} = 1.0 - 0.008i, \quad g_{21} = 0.06 + 0.001i. \tag{10}$$

Regime 2. $\Delta_2 = 2.5 \times 10^6$ s^{-1}, $\Delta_4 = -1.0 \times 10^9$ s^{-1}, $\tau_0 = 7.4 \times 10^{-7}$ s, $c_0 = 1.2$. We obtain $L_{\text{diff}} = 1.26$ cm, $U_0 = 1.6 \times 10^7$ s^{-1}, $V_g/c = 1.4 \times 10^{-5}$, and hence

$$\delta = 1.0, \quad g_d = 1.0 - 0.019i, \quad g_{11} = -1.0 - 0.023i,$$
$$g_{12} = 1.0 + 0.046i, \quad g_{21} = 0.08 + 0.001i. \tag{11}$$

We see that the imaginary parts of the coefficients in Eqs. (9a) and (9b) are indeed much less than their real parts. The physical reason for so small imaginary parts is due to the quantum interference effect induced by the control field that makes the absorption of the probe field largely suppressed. In the following discussion, the small imaginary parts of the coefficients are neglected for analytical analysis, but they are included in numerical simulations. We also see that due to the active character of our resonant atomic system, one can obtain the case of self-focusing ($g_{11} \approx 1$; Regime 1) and the case of self-defocusing ($g_{11} \approx -1$; Regime 2). In this article, we concentrate on the case of self-focusing. The study on the self-defocusing case will be given elsewhere.

We now estimate the self- and cross-Kerr susceptibilities based on the formulas of α_{11} and α_{12} given by Eqs. (B1a) and (B1b) and the system parameters given above. Under the EIT condition $|\Omega_c|^2 \gg \gamma_{31}\gamma_{21}$ [38], we obtain

$$\chi_{pp}^{(3)} = \frac{2c}{\omega_p}\frac{|\mathbf{p}_{13,24}|^2}{\hbar^2}\alpha_{11} \approx 3.57 \times 10^{-9} \ (\text{m/V})^2, \quad (12a)$$

$$\chi_{pa}^{(3)} = \frac{2c}{\omega_p}\frac{|\mathbf{p}_{13,24}|^2}{\hbar^2}\alpha_{12} \approx 2.19 \times 10^{-9} \ (\text{m/V})^2, \quad (12b)$$

which are at least one order of magnitude larger than that without the EIT effect. The giant enhancement of the Kerr coefficients is also due to the quantum interference induced by the control field.

B. Optical bullet solutions and their stability

Equation (9a) without the CPM term (i.e., $g_{12} = 0$) is a $(3+1)$D NLS equation. If in such a case an optical bullet is excited, it will be unstable [4,5]. Our aim is not only to obtain an optical bullet, but also to provide a way to stabilize it. Thus in our model the assisted field interacting resonantly with the energy states $|2\rangle$ and $|4\rangle$ is added (see Fig. 1), which contributes a trapping potential to the probe field and hence can be used to stabilize the optical bullet formed in the probe field.

Since the assisted field (represented by v) is governed by the Helmholtz Eq. (9b), its solution can be obtained independently. Using the transformation $v = \Psi(r)\exp[i(-bs + l\phi)]$ with $r^2 = \xi^2 + \eta^2$, Eq. (9b) with $\delta = 1$ becomes

$$\frac{\partial^2\Psi}{\partial r^2} + \frac{1}{r}\frac{\partial\Psi}{\partial r} + \left(2b - \frac{l^2}{r^2}\right)\Psi = 0, \quad (13)$$

where $l(\geqslant 0)$ is a winding number (or vorticity) and b is a real constant. Considering a natural boundary condition, the solution of Eq. (13) is the Bessel function $\Psi = J_l(\sqrt{2b}r)$, with J_l being the lth-order Bessel function. Substituting this solution into Eq. (9a) with $g_d = 1$, we can obtain the $(3+1)$D NLS equation

$$i\frac{\partial u}{\partial s} + \frac{1}{2}\left(\frac{\partial^2}{\partial\xi^2} + \frac{\partial^2}{\partial\eta^2} + \frac{\partial^2}{\partial\tau^2}\right)u + g_{11}|u|^2u$$
$$+ g'_{12}c_0^2|J_l(\sqrt{2b}r)|^2u = 0, \quad (14)$$

with $g'_{12} = \alpha_{12}/|\alpha_{11}|$. Obviously, the role of the assisted field is to contribute an external trapping potential to the probe field.

Using the further transformation $u = \exp(i\mu s)\psi(\xi,\eta,\tau)$, Eq. (14) becomes

$$\left(\frac{\partial^2}{\partial\xi^2} + \frac{\partial^2}{\partial\eta^2} + \frac{\partial^2}{\partial\tau^2}\right)\psi - 2\mu\psi + 2g_{11}\psi^3$$
$$+ 2c_0^2g'_{12}|J_l(\sqrt{2b}r)|^2\psi = 0, \quad (15)$$

where ψ is a real function and μ is a propagation constant. The optical bullet solutions of Eq. (15) will be presented in the following.

The linear stability of an optical bullet solution will be analyzed by considering a perturbation to the optical bullet ψ, i.e.,

$$u(\xi,\eta,\tau,s) = [\psi + (w_1 + w_2)\exp(\lambda s) + (w_1^* - w_2^*)$$
$$\exp(\lambda^* s)]\exp(i\mu s), \quad (16)$$

where $w_{1,2} = w_{1,2}(\xi,\eta,\tau)$ and λ are the normal modes and corresponding eigenvalue of the perturbation, respectively. Substituting the perturbed solution (16) into Eq. (14), one obtains the linear eigenvalue problem

$$-i\lambda w_1 = \frac{1}{2}\left(\frac{\partial^2}{\partial\xi^2} + \frac{\partial^2}{\partial\eta^2} + \frac{\partial^2}{\partial\tau^2}\right)w_2$$
$$+ \left[-\mu + g_{11}\psi^2 + c_0^2g'_{12}|J_l(\sqrt{2b}r)|^2\right]w_2, \quad (17a)$$

$$-i\lambda w_2 = \frac{1}{2}\left(\frac{\partial^2}{\partial\xi^2} + \frac{\partial^2}{\partial\eta^2} + \frac{\partial^2}{\partial\tau^2}\right)w_1$$
$$+ \left[-\mu + 3g_{11}\psi^2 + c_0^2g'_{12}|J_l(\sqrt{2b}r)|^2\right]w_1, \quad (17b)$$

which can be solved numerically by using the method in Ref. [39]. The optical bullet is stable if the real part of all eigenvalues is negative or zero.

We now present various localized nonlinear solutions of Eq. (15) for different l. For $l = 0$ we obtain a zero-order optical bullet, for which the external potential provided by the assisted field is a trapping potential proportional to $|J_0(\sqrt{2}r)|^2$, where $J_0(\sqrt{2}r)$ is zero-order Bessel function, (we take $b = 1$ without loss of generality). Shown in Figs. 3(a) and 3(b) are the isosurfaces of the amplitude $\psi = 0.01$ of the probe field for $(c_0,\mu) = (1.5,0.7)$ and for $(c_0,\mu) = (2.5,3.3)$, respectively. The solution is obtained by numerically solving Eq. (15) in
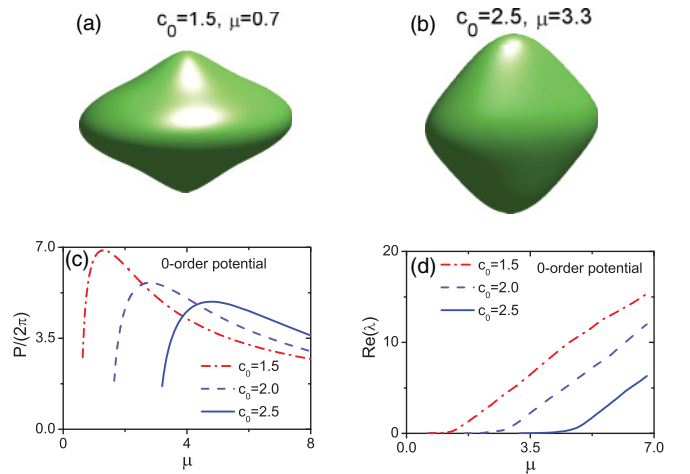

FIG. 3. (Color online) (a) and (b) Isosurface plots of the amplitude $\psi = 0.01$ of the probe field in the self-focusing case (i.e., $g_{11} = 1$, $g_{12} = 1$) for $(c_0,\mu) = (1.5,0.7)$ and $(c_0,\mu) = (2.5,3.3)$, respectively. The external trapping potential contributed by the assisted field is the zero-order (i.e., $l = 0$) Bessel function. (c) Probe-field power P as a function of the propagation constant μ and c_0. (d) Real part of maximum eigenvalue, i.e., $\text{Re}(\lambda)$, as a function of μ and c_0 obtained by solving the eigenvalue problem (17). In both panels (c) and (d), the dotted-dashed, dashed, and solid lines are for $c_0 = 1.5, 2.0$, and 2.5, respectively.

terms of the modified squared-operator method [39]. The initial trial function in the numerical simulation is of a Gaussian type, which evolves into the ground state of Eq. (15), i.e., the optical bullet solution of the system.

To test the stability of the optical bullet obtained, we calculate the power of the probe field, defined by $P = 2\pi \iiint_{-\infty}^{+\infty} \psi^2 d\xi d\eta d\tau$, as a function of the propagation constant μ and the potential strength constant c_0. The result is shown in Fig. 3(c). We see that for a given c_0, P first increases to arrive at a maximum, and then decreases. According to the Vakhitov-Kolokolov (VK) criterion [40], the domain in which the optical bullet is stable is the one with $dP/d\mu > 0$. Generally, the stability domain is small for small c_0. However, when increasing c_0 the stability domain is enlarged. This is easy to understand because a larger c_0 means a stronger trapping of the optical bullet provided by the external potential. Hence, one can adjust the assisted field, and hence the external potential, to control the stability of the optical bullet, which is easy to realize physically in the present active system.

To further check the stability of the optical bullet solutions, we have also numerically solved the eigenvalue problem (17). We employ the Fourier collocation method introduced in Ref. [39] that was developed for one-dimensional (1D) and two-dimensional (2D) problems, but here we extend it to the present 3D one. The real part of maximum eigenvalue, Re(λ), as a function of μ and c_0 has been shown in Fig. 3(d). From the figure we see that the stability domain of the optical bullets [i.e. the domain where Re(λ) is nonpositive] becomes indeed larger when increasing the potential strength c_0.

Shown in Fig. 4 is the result for first-order optical bullets ($l = 1$). In this case, the external potential contributed by the assisted field is proportional to $|J_1(\sqrt{2}r)|^2$, with $J_1(\sqrt{2}r)$ being the first-order Bessel function.
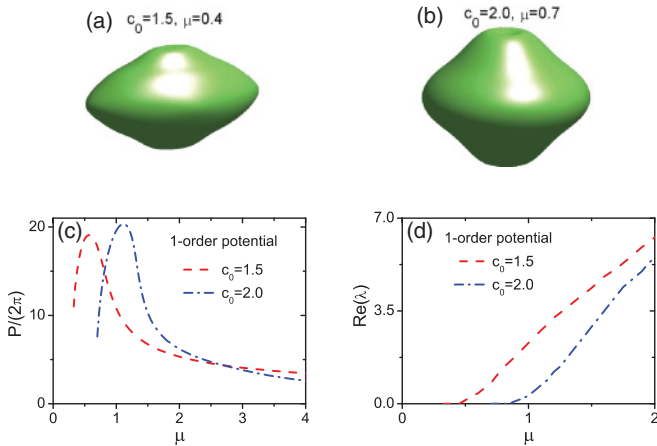
We see that for a given c_0 the stability domain of the first-order optical bullet ($l = 1$) is narrower than that of the zero-order optical bullet ($l = 0$). The reason is that the trap potential given by $|J_1(\sqrt{2}r)|^2$ is weaker than that given by $|J_0(\sqrt{2}r)|^2$, and hence the first-order optical bullet shown in Fig. 4 is less stable than the zero-order optical bullet shown in Fig. 3. In the same way, high-order optical bullet solutions for $l \geqslant 1$ can also be obtained, and their stability domains can also be identified. The stability domains of the high-order optical bullets are more narrow because the strength of the trapping potential with the form $|J_l(\sqrt{2}r)|^2$ becomes more weak as l increases.

The results presented above are the stationary solutions based on the Eq. (15). It is necessary to investigate the time evolution and their stability of the optical bullets starting directly from the evolution Eq. (9a), which has complex coefficients with small imaginary parts. For this aim, we have made a numerical simulation on Eq. (9a) by taking the optical bullet solution ψ of Eq. (15) as an initial condition, and adding a random perturbation to it. Concretely, we take $u(s = 0, \xi, \eta, \tau) = \psi(\xi, \eta, \tau)(1 + \varepsilon f)$, with ψ being the solution given by Eq. (15), ε being a typical amplitude of the perturbation, and f being a random variable uniformly distributed in the interval [0,1]. We find that Eq. (9a) allows indeed optical bullet solutions which are fairly stable for propagating to a long distance. Illustrated in Fig. 5 is the evolution of the optical bullets based on Eq. (9a) by taking $\varepsilon = 0.1$ and the solutions of Eq. (15) as initial conditions. Panel (a) shows the isosurface plots of the optical bullet for $s = 0.0, 0.4, 2.0, 5.3, 5.6$ by taking the result given in Fig. 3(b) as an initial condition. Panel (b) gives the isosurface plots of the optical bullet for $s = 0.0, 0.8, 1.5, 7.7, 9.0$ by taking the result in Fig. 4(b) as an initial condition. We see that despite some transient change of their shape, the optical bullets relax to self-cleaned forms which are quite close to the unperturbed ones.

Since $\tau = (t - z/V_g)/\tau_0$, the propagating velocity of the optical bullets V_{OL} is approximately equal to V_g. We obtain

$$V_{OL} \approx 5.6 \times 10^{-6} c, \qquad (18)$$

The generation power of the $(3 + 1)$D optical bullets can be estimated by calculating Poynting's vector. The peak power of the probe field is given by $\bar{P}_{max} = 2\epsilon_0 c n_p S_0 (\hbar/|\mathbf{p}_{13}|)^2 U_0^2 |u_{max}|^2$, with n_p and S_0 being the reflective index and the cross-section area of the probe beam, respectively. Taking $S_0 = \pi R_\perp^2 \approx 0.5 \times 10^{-4}$ cm^2 and using

FIG. 4. (Color online) (a) and (b) Isosurface plots of the amplitude $\psi = 0.01$ of the probe field in the self-focusing case (i.e., $g_{11} = 1$, $g_{12} = 1$) for $(c_0, \mu) = (1.5, 0.4)$ and $(c_0, \mu) = (2.0, 0.7)$, respectively. The external trapping potential contributed by the assisted field is the first-order (i.e., $l = 1$) Bessel function. (c) Probe-field power P as a function of the propagation constant μ and c_0. (d) Real part of the maximum eigenvalue, i.e., Re(λ), as a function of μ and c_0 obtained by solving the eigenvalue problem (17). In both panels (c) and (d), the dashed and dotted-dashed lines are for $c_0 = 1.5$ and 2.0, respectively.
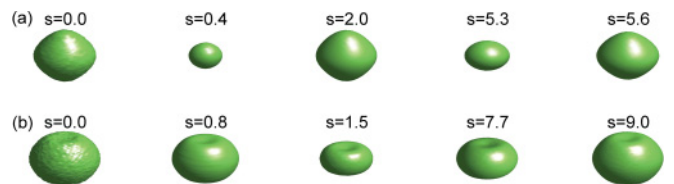

FIG. 5. (Color online) Evolution of optical bullets based on Eq. (9a) by taking the solutions of Eq. (15) as initial conditions. (a) Isosurface plots of the optical bullet for $s = 0.0, 0.4, 2.0, 5.3, 5.6$ by taking the result in Fig. 3(b) as an initial condition. (b) Isosurface plots of the optical bullet for $s = 0.0, 0.8, 1.5, 7.7, 9.0$ by taking the result in Fig. 4(b) as an initial condition.

the other parameters given above, we obtain the generation power of the optical bullets

$$\bar{P}_{\max} \approx 0.01 \ \mu W \qquad (19)$$

(or corresponding input energy 1.48×10^{-14} J). Consequently, the $(3 + 1)$D optical bullets obtained in the present system have ultraslow propagating velocity and very low generation power, which are very different from the other generation schemes where the optical bullets have the propagating velocity not far from c and their generation power up to a megawatt is usually needed [9,17].

V. DISCUSSION AND SUMMARY

In the study given above, we have assumed the control field Rabi frequency Ω_c is a constant during time evolution. In a real experiment, Ω_c can not be too strong and hence will have a small depletion after an optical bullet propagates to a long distance. In this situation it is necessary to consider the evolution of Ω_c, like that done in Refs. [41,42]. This is an interesting topic deserving to be investigated further.

In summary, we have proposed a scheme for generating stable ultraslow optical bullets at very low light level via atomic coherence. The system we considered is an ensemble of resonant, lifetime-broadened four-state atoms with an N-type level configuration, working in the EIT regime. Due to the quantum interference effect induced by the control field, the absorption of the probe field is largely suppressed. Furthermore, the Kerr nonlinearity is greatly enhanced and the dispersion property of the probe field is drastically changed. By using the method of multiple scales we have derived two coupled nonlinear envelope equations governing the evolution of the envelopes of the probe and the assisted fields. We have

shown that by choosing suitable atomic levels and by using a CW assisted field or a pulsed assisted one with a large time length, the envelope equation of the probe field is reduced into a $(3 + 1)$D NLS equation and the envelope of the assisted field is reduced into a linear Helmholtz equation. We have obtained various optical bullet solutions for the probe-field envelope and demonstrated that such optical bullets have many novel features, including very slow propagating velocity and very low generation power. Moreover, they can be actively controlled and manipulated by adjusting system parameters. The stabilization of such optical bullets can be easily realized by means of the linear trapping potential provided by the assisted field. The stability of the optical bullets has also been investigated in detail by using the VK criterion and linear stability analysis. The results presented here may be useful for understanding the physical properties of coherent atomic systems and guiding experimental findings of $(3 + 1)$D nonlinear excitations with very low generation power, which may have potential applications in optical information processing and transmission.

APPENDIX A: EQUATIONS OF MOTION FOR σ_{ij}

Equations of motion for σ_{ij} are given by

$$i\frac{\partial}{\partial t}\sigma_{11} - i\Gamma_{31}\sigma_{33} + \Omega_p^*\sigma_{31} - \Omega_p\sigma_{31}^* = 0, \qquad (A1a)$$

$$i\frac{\partial}{\partial t}\sigma_{22} - i\Gamma_{32}\sigma_{33} - i\Gamma_{42}\sigma_{44} + \Omega_c^*\sigma_{32} - \Omega_c\sigma_{32}^* + \Omega_a^*\sigma_{42} - \Omega_a\sigma_{42}^* = 0, \qquad (A1b)$$

$$i\left(\frac{\partial}{\partial t} + \Gamma_3\right)\sigma_{33} - \Omega_p^*\sigma_{31} + \Omega_p\sigma_{31}^* - \Omega_c^*\sigma_{32} + \Omega_c\sigma_{32}^* = 0, \qquad (A1c)$$

$$i\left(\frac{\partial}{\partial t} + \Gamma_4\right)\sigma_{44} - \Omega_a^*\sigma_{42} + \Omega_a\sigma_{42}^* = 0, \qquad (A1d)$$

$$\left(i\frac{\partial}{\partial t} + d_{21}\right)\sigma_{21} + \Omega_c^*\sigma_{31} + \Omega_a^*\sigma_{41} - \Omega_p\sigma_{32}^* = 0, \qquad (A1e)$$

$$\left(i\frac{\partial}{\partial t} + d_{31}\right)\sigma_{31} + \Omega_p(\sigma_{11} - \sigma_{33}) + \Omega_c\sigma_{21} = 0, \qquad (A1f)$$

$$\left(i\frac{\partial}{\partial t} + d_{41}\right)\sigma_{41} + \Omega_a\sigma_{21} - \Omega_p\sigma_{43} = 0, \qquad (A1g)$$

$$\left(i\frac{\partial}{\partial t} + d_{32}\right)\sigma_{32} + \Omega_c(\sigma_{22} - \sigma_{33}) + \Omega_p\sigma_{21}^* - \Omega_a\sigma_{43}^* = 0, \qquad (A1h)$$

$$\left(i\frac{\partial}{\partial t} + d_{42}\right)\sigma_{42} + \Omega_a(\sigma_{22} - \sigma_{44}) - \Omega_c\sigma_{43} = 0, \qquad (A1i)$$

$$\left(i\frac{\partial}{\partial t} + d_{43}\right)\sigma_{43} + \Omega_a\sigma_{32}^* - \Omega_p^*\sigma_{41} - \Omega_c^*\sigma_{42} = 0, \qquad (A1j)$$

where Γ_{ij} is the rate at which population decays from the state $|i\rangle$ to the state $|j\rangle$, and $d_{ij} = \Delta_i - \Delta_j + i\gamma_{ij}$ with $\gamma_{ij} \equiv (\Gamma_i + \Gamma_j)/2 + \gamma_{ij}^{\text{dph}}$. Here $\Gamma_i = \sum_{E_j < E_i} \Gamma_{ij}$ and γ_{ij}^{col} denotes the dipole dephasing rate caused by atomic collisions.

APPENDIX B: EXPLICIT EXPRESSIONS OF α_{jl}

The explicit expressions of α_{jl} read

$$\alpha_{11} = \frac{\kappa_{13}}{D} \left\{ \Omega_c a_{32}^{*(2)} - (\omega + d_{21}) \left[\frac{4}{\Gamma_{31}} \text{Im}\left(\frac{d_{21}}{D}\right) + a_{22}^{(2)} \right] \right\}, \tag{B1a}$$

$$\alpha_{12} = -\frac{\kappa_{13}|\Omega_c|^2}{(\omega + d_{41})D^2} \tag{B1b}$$

$$\alpha_{21} = \frac{\kappa_{24}}{|\Omega_c|^2 - d_{42}d_{43}} \left[d_{43}a_{22}^{(2)} + \Omega_c a_{32}^{*(2)} - \frac{|\Omega_c|^2}{(\omega + d_{41})D} \right], \tag{B1c}$$

with

$$a_{22}^{(2)} = \left[\frac{2}{\Gamma_{31}}\text{Im}\left(\frac{d_{21}}{D}\right) - \frac{\text{Im}\left(\frac{1}{d_{32}^* D}\right)}{\text{Im}\left(\frac{1}{d_{32}}\right)} - \frac{\Gamma_{32}}{\Gamma_{31}|\Omega_c|^2}\frac{\text{Im}\left(\frac{d_{21}}{D}\right)}{\text{Im}\left(\frac{1}{d_{32}}\right)} \right], \tag{B2a}$$

$$a_{33}^{(2)} = \frac{2\text{Im}\left(\frac{d_{21}}{D}\right)}{\Gamma_{31}}, \tag{B2b}$$

$$a_{32}^{(2)} = \frac{1}{d_{32}} \left[\frac{\Omega_c}{D^*} + \Omega_c(a_{33}^{(2)} - a_{22}^{(2)}) \right]. \tag{B2c}$$

[1] Y. Silberberg, Opt. Lett. **22**, 1282 (1990).

[2] L. Berge, Phys. Rep. **303**, 260 (1998).

[3] Y. S. Kivshar and D. E. Pelinovsky, Phys. Rep. **331**, 117 (1998).

[4] B. A. Malomed, D. Mihalache, F. Wise, and L. Torner, J. Phys. B **7**, R53 (2005), and references therein.

[5] Y. S. Kivshar and G. P. Agrawal, *Optical Solitons: From Fibers to Photonic Crystals* (Academic Press, London, 2006), and references therein.

[6] X. Liu, L. J. Qian, and F. W. Wise, Phys. Rev. Lett. **82**, 4631 (1999).

[7] M. Blaauboer, B. A. Malomed, and G. Kurizki, Phys. Rev. Lett. **84**, 1906 (2000).

[8] I. N. Towers, B. A. Malomed, and F. W. Wise, Phys. Rev. Lett. **90**, 123902 (2003).

[9] P. Di Trapani, G. Valiulis, A. Piskarskas, O. Jedrkiewicz, J. Trull, C. Conti, and S. Trillo, Phys. Rev. Lett. **91**, 093904 (2003).

[10] D. Mihalache, D. Mazilu, F. Lederer, B. A. Malomed, Y. V. Kartashov, L.-C. Crasovan, and L. Torner, Phys. Rev. Lett. **95**, 023902 (2005).

[11] M. Matuszewski, E. Infeld, B. A. Malomed, and M. Trippenbach, Phys. Rev. Lett. **95**, 050403 (2005).

[12] L. Bergé and S. Skupin, Phys. Rev. Lett. **100**, 113902 (2008).

[13] M. Belić, N. Petrović, W. P. Zhong, R. H. Xie, and G. Chen, Phys. Rev. Lett. **101**, 123904 (2008).

[14] I. B. Burgess, M. Peccianti, G. Assanto, and R. Morandotti, Phys. Rev. Lett. **102**, 203903 (2009).

[15] S. H. Chen and J. M. Dudley, Phys. Rev. Lett. **102**, 233903 (2009).

[16] D. Abdollahpour, S. Suntsov, D. G. Papazoglou, and S. Tzortzakis, Phys. Rev. Lett. **105**, 253901 (2010).

[17] S. Minardi, F. Eilenberger, Y. V. Kartashov, A. Szameit, U. Röpke, J. Kobelke, K. Schuster, H. Bartelt, S. Nolte, L. Torner, F. Lederer, A. Tünnermann, and T. Pertsch, Phys. Rev. Lett. **105**, 263901 (2010).

[18] A. Muñoz Mateo, V. Delgado, and B. A. Malomed, Phys. Rev. A **82**, 053606 (2010).

[19] Y. V. Kartashov, B. A. Malomed, and L. Torner, Rev. Mod. Phys. **83**, 247 (2011).

[20] D. Mihalache, D. Mazilu, F. Lederer, and Y. S. Kivshar, Opt. Lett. **32**, 3173 (2007).

[21] D. Mihalache, D. Mazilu, F. Lederer, and Y. S. Kivshar, Phys. Rev. A **79**, 013811 (2009).

[22] D. Mihalache, J. Optoelectron. Adv. M. **12**, 12 (2010).

[23] M. Fleischhauer, A. Imamoglu, and J. P. Marangos, Rev. Mod. Phys. **77**, 633 (2005), and references therein.

[24] Y. Wu and L. Deng, Phys. Rev. Lett. **93**, 143904 (2004).

[25] G. Huang, L. Deng, and M. G. Payne, Phys. Rev. E **72**, 016617 (2005).

[26] C. Hang and G. Huang, Phys. Rev. A **77**, 033830 (2008).

[27] W.-X. Yang, A.-X. Chen, L.-G. Si, K. Jiang, X. Yang, and R.-K. Lee, Phys. Rev. A **81**, 023814 (2010).

[28] T. Hong, Phys. Rev. Lett. **90**, 183901 (2003).

[29] H. Michinel, M. J. Paz-Alonso, and V. M. Perez-Garcia, Phys. Rev. Lett. **96**, 023903 (2006).

[30] C. Hang, G. Huang, and L. Deng, Phys. Rev. E **74**, 046601 (2006).

[31] C. Hang, V. V. Konotop, and G. Huang, Phys. Rev. A **79**, 033826 (2009).

[32] Here the first "3" refers to spatial coordinates and "1" refers one time coordinate.

[33] D. A. Steck, Rubidium 87 D Line Data [http://steck.us/alkalidata/].

[34] H. J. Li, L. W. Dong, C. Hang, and G. Huang, Phys. Rev. A **83**, 023816 (2011).

[35] A. Jeffery and T. Kawahara, *Asymptotic Methods in Nonlinear Wave Theory* (Pitman, London, 1982).

[36] The frequency and wave vector of the probe field are given by $\omega_p + \omega$ and $k_p + K_p(\omega)$, respectively. Thus $\omega = 0$ corresponds to the center frequency of the probe field.

[37] In order to make the probe field have a long enough time interacting with the assisted field, the pulse length of the assisted field τ_a must satisfy $L/V_g \leqslant \tau_a$, where L is the length of the atomic medium.

[38] L. Li and G. Huang, Phys. Rev. A **82**, 023809 (2010).

[39] J. Yang, *Nonlinear Waves in Integrable and Nonintegrable Systems* (SIAM, Philadelphia, 2011).

[40] M. G. Vakhitov and A. A. Kolokolov, Sov. J. Radiophys. Quantum Electron. **16**, 783 (1973).

[41] A. Alexandrescu, H. Michinel, and V. M. Pérez-García, Phys. Rev. A **79**, 013833 (2009).

[42] A. Alexandrescu, A. Bueno-Orovio, J. R. Salgueiro, and V. M. Pérez-Garcia, Comput. Phys. Commun. **180**, 912 (2009).